



What do spore particles look like - use of real-time measurements and holography imaging to view spore particles from four bioaerosol generators

Clara-E Pogner, Elias Graf, Erny Niederberger & Markus Gorfer

To cite this article: Clara-E Pogner, Elias Graf, Erny Niederberger & Markus Gorfer (2024) What do spore particles look like - use of real-time measurements and holography imaging to view spore particles from four bioaerosol generators, *Aerosol Science and Technology*, 58:7, 779-795, DOI: [10.1080/02786826.2024.2338544](https://doi.org/10.1080/02786826.2024.2338544)

To link to this article: <https://doi.org/10.1080/02786826.2024.2338544>

 [View supplementary material](#) 

 Published online: 25 Apr 2024.

 [Submit your article to this journal](#) 

 Article views: 118

 [View related articles](#) 

 [View Crossmark data](#) 



What do spore particles look like - use of real-time measurements and holography imaging to view spore particles from four bioaerosol generators

Clara-E Pogner^a, Elias Graf^b, Erny Niederberger^b, and Markus Gorfer^a

^aCenter for Health & Bioresources, AIT Austrian Institute of Technology GmbH, Tulln, Austria; ^bSwisens AG, Emmen, Luzern, Switzerland

ABSTRACT

To study bioaerosols under controlled conditions, aerosol chambers equipped with aerosol generators have been used for a long time. The method used for generation can change the constitution and properties of the bioaerosol produced, including the viability of fungal spores, bacteria or airborne viruses. The properties of a bioaerosol in turn influence the results of detection and enumeration methods downstream. To evaluate and compare bioaerosol generators, previous methods provided either real-time data without particle characterization, relied on labor-intensive microscopy or used culturing, which has high variability. In our study, we used the novel instrument SwisensPoleno Jupiter, providing real-time enumeration and subsequent bioaerosols characterization through holographic image analysis. With this tool, we investigated the characteristics of bioaerosols produced by four different aerosol generators using fungal spores from *Aspergillus brasiliensis*, *Cladosporium cladosporioides* and *Trichoderma longibrachiatum* in controlled chamber environments. The rotating brush generator (RBG) produce small, round particles for *A. brasiliensis*, between 5 and 15 μm , while the fungal aerosol generator (FAG) released small particles for *C. cladosporioides* and *T. longibrachiatum*. Conversely, the SwisensAtomizer (SWA) produced larger non-spherical particles, likely spore aggregates, and the liquid sparging aerosolizer (LSA), exhibited a high portion of datapoints with empty images, supposedly water droplets. All generators showed a wide range of particle sizes. Holographic image analysis revealed that the choice of bioaerosol generator had a significant influence on the constitution of produced aerosols, in terms of proportions of single spores, chains and agglomerates, emphasizing the importance to select the bioaerosol generator depending on the desired aerosol.

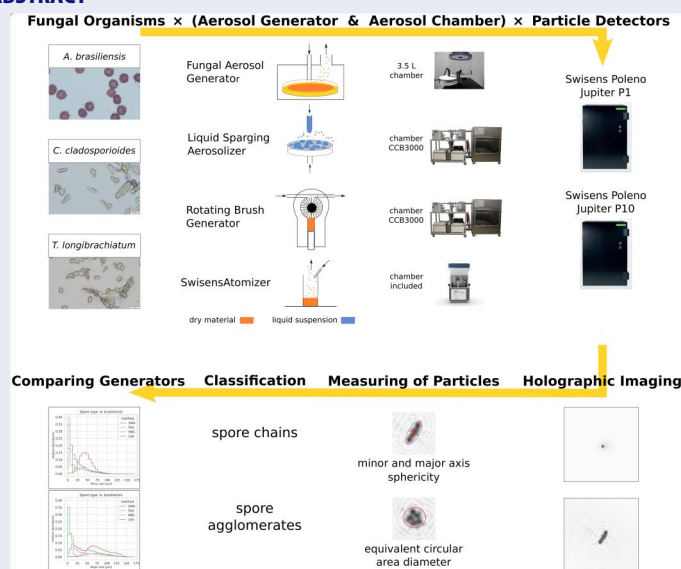
ARTICLE HISTORY

Received 20 November 2023
Accepted 9 March 2024

EDITOR

Hans Moosmüller

GRAPHICAL ABSTRACT



CONTACT Clara-E Pogner ✉ clara.pogner@ait.ac.at 📍 Center for Health & Bioresources, AIT Austrian Institute of Technology GmbH, Konrad-Lorenz-Straße 24, Tulln, 3430 Austria.

📄 Supplemental data for this article can be accessed online at <https://doi.org/10.1080/02786826.2024.2338544>.

© 2024 American Association for Aerosol Research

1. Introduction

Small-sized biological material in air, so-called bioaerosols, consisting mainly of pollen, fungal spores, bacteria and viruses, have an impact on human life in various areas. Bioaerosols are generated by man-made or natural particle emissions, and can affect the health of humans, animals and plants by illnesses like allergies or infections. Therefore most studies about bioaerosols focus on their negative effects, for example on air quality (Górny et al. 2002; Hasegawa, Yamasaki, and Horiguchi 2011; Yamamoto et al. 2012; Heo, Kim, and Lee 2014; Unterwurzacher et al. 2018), human health (Douwes et al. 2003; Liebers, Raulf-Heimsoth, and Brüning 2008; Kim, Kabir, and Jahan 2018), health risks, and disease development and prevention (Soler and Schlosser 2012; Viegas et al. 2015; Oteros et al. 2019). Bioaerosols also play an important role in damp buildings (Gunnbjörnsdottir et al. 2003; Mudarri and Fisk 2007), hospital hygiene concepts (Stockwell et al. 2019) and safety and security of pharmaceutical products as well as food (European Commission 2008; Masotti et al. 2019; Theisinger, De Smidt, and Lues 2021). The state of knowledge about these particles in the air around us is limited. For the impact on human health, dose-response relationships are still not or not fully understood. Therefore, the improvement of the available data is a focus point to better understand exposure and thus the dose involved in negative health effects (Walser-Reichenbach et al. 2020). The reason for the poor state of knowledge is that measuring such particles in the air with conventional measuring methods is, on the one hand, very time-consuming and thus expensive and, on the other hand, involves a time delay. For the areas of hospitals, food and pharma safety, detection of any organism that can lead to negative health effects or to contamination of the product is essential (Douwes et al. 2003). As the detection and classification of bioaerosols is important in these areas, a variety of sampling and analysis techniques have been developed over the years (Ghosh, Lal, and Srivastava 2015).

To test and validate established as well as newly developed bioaerosol sampling instruments and analytical methods, measurements under controlled laboratory conditions are performed. In some countries such efficiency and performance characterization of instruments are already mandatory, and the experimental design and used equipment are defined in standards (CEN/TC 137/WG5, 2021). An overview of commonly used chambers and bioaerosol generators used in these artificial setups is given by Pogner

et al.'s (2019) supplementary section. The setups focus on reproducible, well defined aerosols and stable conditions, often with single spore particles or small aerosols. However, in real live environments bioaerosols are produced by different mechanisms (Alsved et al. 2020), and fungal spores often develop in aggregates (e.g., as conidial chains from the hyphal network), but are normally released in single units to the atmosphere (Madsen et al. 2016). In development of bioaerosol generation methods, the focus has been laid on different properties, such as producing high concentration, generate particles with the same properties as in the final application or influence the viability as little as possible (Mainelis et al. 2005; Jung et al. 2009; Scheermeyer and Agranovski 2009; Lee et al. 2010; Simon and Duquenne 2013; Madsen et al. 2016). An overview of different technologies used for bioaerosol generation from liquids, powders and colonies is given by Alsved et al. 2020, while investigations of the generators effect on cultivability of fungal spores and bacteria have been done in experimental studies such as Löndahl et al. 2012; Zhen et al. 2014; Danelli et al. 2021. For these comparisons, a method for measuring and describing the particles properties has to be used. All evaluations are therefore based and influenced by the chosen detection method. Most of the time analytical techniques are used that give a result after a certain sampling time, for example sampling onto filters for microscopy or into liquid for culturing (Scheermeyer and Agranovski 2009; Zhen et al. 2014). Most of the used techniques rely on active sampling into or onto a medium or surface, leading to delays between sampling and result, potential change in particle properties (e.g., dissolution of agglomerates), and only momentary or sparse data from long sampling periods. This is especially noticeable for high-throughput sequencing techniques, which provide an excellent taxonomic resolution at the expense of temporal and spatial resolution (Ghosh, Lal, and Srivastava 2015). In outdoor air the volumetric Hirst method is widely used for detection of pollen and bigger fungal spores (Hirst 1952). Typically, individual particles are collected and identified by a trained person. This results in lower specificity, compared to next-generation sequencing techniques, but immediate availability and time resolved monitoring. In many cases also optical particle counters are used, that give the particle number and size distribution as real-time data, but provide no distinction between biological and non-biological particles (Pogner et al. 2019). Newly developed bioaerosol real-time monitoring instruments may solve some of these issues, as the data is available

immediately and continuously over a long period of time (Huffman et al. 2020). The instruments provide the characteristics of the individual particles in real time and also identify a selection of particle types, for example, by automatic pollen identification (Buters et al. 2022). The classification can be done with the help of supervised machine learning, where an algorithm learns to distinguish between certain particle classes, on the basis of labeled datasets. Real time classification of pollen has previously been shown feasible (Tummon et al. 2021), and also potential for detection of fungal spores (Erb et al. 2023). But most fungal spores have considerably smaller size and less pronounced surface characters than *Alternaria* and could be a major challenge for real time classification.

The goal of the study presented here was to compare different bioaerosol generators to each other, by using state of the art, real-time aerosol characterization methods. To achieve detailed descriptions and characterization of the produced fungal bioaerosols, the SwisensPoleno Jupiter was used. This instrument makes use of holographic image analysis that allows real time classification and counting of airborne particles in the size range of fungal spores. Assessment of selected morphological characteristics such as size, shape and surface properties together with UV autofluorescence detection provides an increased resolution of fungal spore types and allows distinction from non-fungal particles. A detailed description of the instrument is provided in Sauvageat et al. (2020). Through the obtained imaging data and the following analysis of the produced bioaerosols, the range of application of the tested aerosol generators can be described, depending on which kind of aerosols the laboratory studies is aiming on.

We hypothesized that nebulization from liquid suspensions would create differences in particle characteristics compared to aerosolization from solid sources. Additionally, distinct effects from different dust aerosolization techniques were expected on the ratio of aggregates to spore chains.

2. Material and methods

To test and validate established as well as newly developed bioaerosol generators under controlled laboratory conditions, a new detection and characterization method was used. In the study presented here, we compared bioaerosol generators using an air-flow cytometer for real-time bioaerosol identification, the SwisensPoleno Jupiter. In contrast to optical particle counters, the system uses holographic images of the

detected particles to analyze their size and morphology, which enables further investigation of the composition of the generated bioaerosol. With this data we were able to evaluate the generated bioaerosols regarding their steady output, particle size, particle shape, as well as combinations of these parameters. The fluorescence and polarization measurement results from SwisensPoleno Jupiter were not used for this study.

2.1. Bioaerosol generators

Four aerosol generators with different methods of aerosolization were tested in this study. Based on the classification of Alsved et al. 2020 the used methods can be described as powder dispersion (SwisensAtomizer, SWA), agar plate dispersion (fungal aerosol generator, FAG), rotating brush (rotating brush generator, RBG) and bubble bursting (liquid sparging aerosolizer, LSA). Two generators operate with dry material (dust; SWA and RBG), one emits the particles directly from fungal colonies (FAG) and one uses liquid suspensions as primary material (LSA).

2.1.1. RBG1000

The rotating brush generator RBG1000 (Palas GmbH, DE; abbreviated “RBG”) is designed to disperse dry material provided in a cylinder. The cylinder is prepared by filling in and gently pressing the fungal material layer by layer. During aerosolization, the cylinder is moved upward toward the rotating brush. The brush then collects material from its bottom side and transports the dust to the upper side, where compressed air blows the dust from the brush into the outlet tube. The RBG is able to produce high concentrations of aerosols. Within this study the material was supplied with the lowest possible feed rate of 1 mm/h, the airflow was set to 1 bar, the rotation of the brush was set to 1200 rpm. The generator was connected to the aerosol chamber CCB3000 (Pogner et al. 2019).

2.1.2. SwisensAtomizer

The SwisensAtomizer (Swisens AG, CH; abbreviated “SWA”) aerosolizes dry material, which is provided in a 2.5 mL macro cuvette (Pastibrand). The cuvette is placed on a vibrational membrane which loosens up the sample with an adjustable vibration frequency and amplitude. The loose particles are then transported away by a slight air stream which is guided into the cuvette. The cuvette and membrane are enclosed in a

small chamber outfitted with a HEPA filter at the air inlet. After dispersion the aerosolized particles need to be actively absorbed by the measuring instrument connected to the SWA outlet, which is designed to directly fit onto the inlet of the SwisensPoleno Jupiter.

2.1.3. Fungal bioaerosol generator

The fungal bioaerosol generator (constructed by Swisens AG, CH; abbreviated “FAG”) was first described by Lee and his team (Lee et al. 2010) for aerosolization of fungal spores directly from a petri dish. The version used in this study was constructed by the Swisens AG following the design of Lee and his team. It consists of two chambers, with the first being only slightly bigger than the petri dish itself, with an inlet for compressed air at the center. The inlet guides the airstream through six horizontal nozzles with a diameter of 0.7 mm. The aerosolized particles are led into a second chamber for distribution and dilution, which is directly attached to the inlet of the SwisensPoleno Jupiter. The second chamber has a volume of 3.4 L and a HEPA filtered fresh air inlet, in order to prevent excessive over or under pressure at the instrument input. The aerosolization can be influenced by the volume flow rate of compressed air of the first chamber, which changes the velocity across the petri dish. It is known that the share of size categories and form classes can be influenced by the speed, the air flows across the colony (Lee et al. 2010). In this study the airflow was set to 750 – 1000 L/h.

2.1.4. Liquid sparging aerosolizer

For the production of bioaerosols from liquid spore suspensions, the Liquid Sparging Aerosolizer (CH Technologies, USA; abbreviated “LSA”) was used, which enables gentle aerosolization and low impact on the cell integrity and viability (Mainelis et al. 2005; Zhen et al. 2014). Aerosols are produced in a low concentration range of several hundred particles per cubic meter by transportation of the suspension onto a porous disk (\varnothing 2.54 cm, stainless steel, 0.2 mm pore size) by a peristaltic pump (PP 3000 C, VWR) and channeling compressed air through the disk to create bursting bubbles and release of aerosols. The suspension needs to be stirred (topolino, IKA) to keep the suspension homogenous throughout the experiment. Only a portion of the suspension is aerosolized and further transported, while the majority is collected at the bottom of the LSA. In this study the airflow of compressed air was adjusted to 750 L/h, the supply of

liquid set to 1 mL/min and the generator connected to the aerosol chamber CCB3000 (Pogner et al. 2019).

2.2. Test material

2.2.1. Organisms

As test organisms, three fungal species were chosen for this study, as they belong to common airborne genera (Li, Liu, and Yao 2022). They were reviewed for their taxonomy by sequencing the ITS and Beta-tubulin region of their DNA. *Aspergillus brasiliensis* (strain DSM 1988) was selected as it is a typical test organism in biotechnological and spore aerosolization studies. *Aspergillus* species are important in various health effects associated with bioaerosols and are very common in indoor air and occupational settings (Sharpe et al. 2013). The conidiospores of *Aspergillus brasiliensis* are black and round and have with a diameter of 3.5 to 4.5 μm . *Cladosporium cladosporioides* (strain F1186) belongs to one of the most abundant genera in outdoor air (Dannemiller et al. 2014). The species is associated with plant decay (Bensch et al. 2010) and therefore also detectable indoors where a lot of plants are accumulated. Conidiospores are brown-green, smooth, conical formed and have a size of 3–3.5 \times 2.5–3 μm . *Trichoderma longibrachiatum* (strain L20) was selected as a health relevant species found indoors and outdoors. It is commonly found in soil and on decaying plant and mushroom material and has a worldwide distribution with a preference for warmer climates (Druzhinina et al. 2008; Samuels et al. 2012). *T. longibrachiatum* is frequently found in water-damaged buildings and is one of the leading sources of emerging human mycoses (Thrane et al. 2001; Hatvani et al. 2019). The conidiospores are green, round, smooth and have a size of 3.5–5 \times 2–3 μm . *Aspergillus brasiliensis* was purchased from the DSM strain collection, the other two species are from air sample isolates and belong to the AIT strain collection.

2.2.2. Cultivation and preparation

As the methods for aerosol production are different for the tested aerosol generators, the starting material needs to be produced in different ways. For the FAG, petri dishes filled with malt extract agar (MEA, Merck Millipore GmbH, USA) were inoculated with fungal spores and incubated for 7 to 14 days at room temperature. The fully grown plates were directly inserted in the FAG. To produce spore suspensions for the LSA, fully grown fungal plates were harvested by scraping the spores off the surface of the agar medium

with a metal spatula. The spores were placed into phosphate-buffered saline (PBS, pH 7.5; 11.5 g Na₂HPO₄, 2.96 g NaH₂PO₄, 5.84 g NaCl, 1 L deionized water) with Tween 20 (Sigma-Aldrich, USA) to a final concentration of 0.01%. Spores were separated from mycelia by vortexing and filtering through sterile glass wool (extra fine, Karl Hecht, DE), placed in a 10-ml-syringe. The suspension was diluted to a concentration of about 10⁷ spores/mL. The final concentration was determined by counting cells in a Neubauer-improved counting chamber (C-Chip, INCYTO Co, KR). For the production of fungal spore dust from *Cladosporium* or *Trichoderma*, fungal plates were harvested by the use of a metal spatula. Instead of a buffer, deionized water was used to create a suspension. After filtration, the suspension was frozen and the spores subsequently freeze dried (Alpha 2-4 LSC, Christ, DE). *Aspergillus brasiliensis* can be harvested by inverting the petri dish onto a clean aluminum foil. By tapping onto the bottom or gently streaking with a metal spatula over the surface of the plate, the spores are loosened from the mycelia and collected on the foil. No further preparation steps were necessary. The dry spores were stored until use and then either filled loosely into a cuvette (SWA) or carefully pressed into a cone (RBG).

2.3. Aerosol chambers

Two of the aerosol generators, the SWA and the FAG, are a combination of an aerosol generator and a mixing chamber, where the produced aerosol is diluted in the air of the mixing chamber. The airstream in the two cases is produced by the aerosolization airflow and the airflow of the SwisensPoleno Jupiter, which draws air from the chambers. The air in the chambers is replaced by the outside air entering the mixing chamber through HEPA filters (DC29, Dyson DE). The LSA and RBG are designed to be connected to a separate aerosol chamber. In this study the test facility CCB3000 (Palas GmbH; Konlechner, et al. 2013) at AIT was used, which comprises of a chamber and a setup to produce a constant airstream. It has HEPA filters at the inlet and the outlet, and a radial compressor providing an airflow of 70 m³/h. The aerosol is injected into the airstream before it enters the chamber unit, which has a total volume of 1.2 m³ (0.53 m³ in the measurement area). One SwisensPoleno Jupiter instruments was placed inside the chamber. Due to the size of the chamber, it was also possible to position a light scattering particle spectrometer (11-C, Grimm Durag

AG, DE) inside, and compare the results of the two instruments.

2.4. Particle measurement instruments

To characterize, measure and further analyze the particles produced by the four aerosol generators, the real-time monitoring system SwisensPoleno Jupiter (Swisens AG, CH) was used (Sauvageat et al. 2020). It can determine many independent features of the aerosol particles using airflow cytometry based on the measurement of light scattering, holographic images, UV-induced fluorescence and polarization. An aerosol-concentrator with a particle size dependent concentration factor of up to 1000 for particles > 10 μm enables a volume flow rate of 40 L/min to be analyzed, resulting in high time resolution of the measurements. Size and morphological feature information of each individual particle is derived from high-resolution digital holography, yielding images from two sides of the particles by two 90° displaced cameras (Figure 1). The advantages of holography include a wide field of view in x, y and z-axes while maintaining a high resolution. This is achieved by capturing the diffraction pattern generated by the particle, and then focusing and reconstructing the particle's image. In addition to the images themselves, the SwisensPoleno Jupiter provides various image processing features, such as calculating the particle area, the eccentricity, the minor and major axis of an ellipse with the same normalized central moments as the particle, and the minimal, mean and maximal grayscale intensity of the particle on each holographic image. The time-resolved measurement of the vertical and horizontal polarized scattered light provides information related to the surface structure, size and the refractive index, allowing for an elaborate particle characterization. With SwisensPoleno Jupiter particles in the range of 0.5 to 300 μm can be detected and measured. However, the image resolution of 0.595 μm per pixel limits the minimum particle size at which the holography can still accurately detect and image the particles to approx. 2 μm.

In the CCB3000 an 11-C (Grimm Durag AG, DE) light scattering particle spectrometer was used to evaluate the particle concentration. The particles in a size range of 0.25 to 32 μm are measured in 31 size channels, at a flow rate of 1.2 L/min. The data is produced as particle number concentration in the different size ranges. No further characterization of the particles is possible with this method.

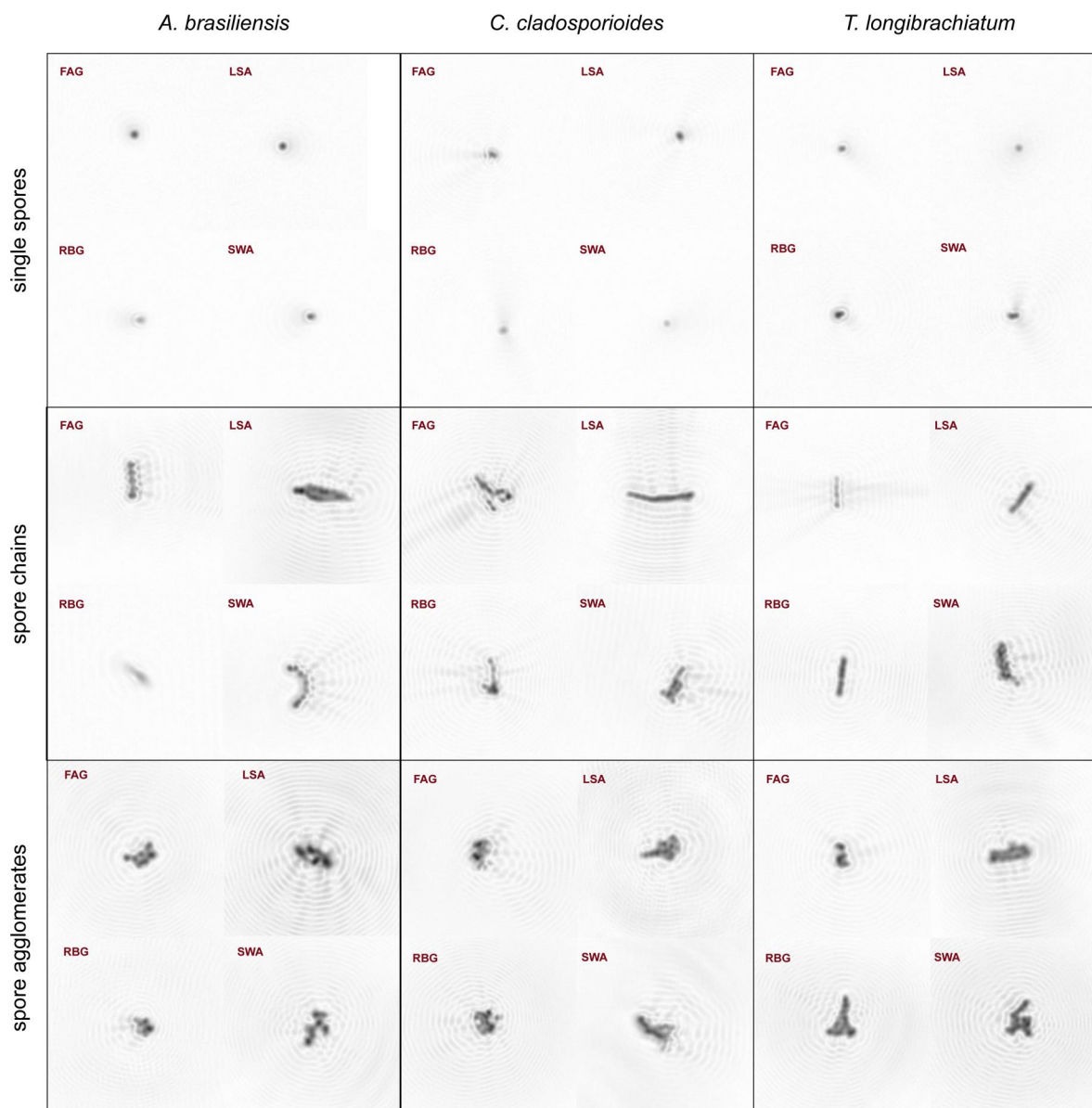


Figure 1. Examples of holographic images of different spore particles categories, for three test organisms aerosolized with different aerosol generators and recorded by SwisensPoleno Jupiter; SWA = SwisensAtomizer, FAG = fungal aerosol generator, RBG = rotating brush generator, LSA = liquid sparging aerosolizer.

2.5. Experimental setup/design

Each of the aerosol generators was tested with all three organisms. To direct the airflow from generator to the measurement instrument, either a SwisensPoleno Jupiter was placed side-by-side with the 11-C in the CCB3000 (LSA, RBG) or the aerosol generator (FAG, SWA) was placed directly on top of the SwisensPoleno Jupiter. All experiments were repeated with two SwisensPoleno Jupiter (P1, P10), which were built with the same components and used the same software. For each combination of test organism, aerosol generator and instrument, at least 6000 data points with recognized particles were collected. Depending on the used aerosol generation

method, different concentrations of particles could be reached. Therefore, also the time to receive the required amount of measurement events was different.

During the laboratory experiments, the instruments were regularly checked to ensure a correctly aligned laser beam and particle stream, as this can be altered by vibrations, which can occur by frequent transportation of the instrument in and out of the CCB3000 chamber.

2.6. Data analysis

To calculate the size of the particles, recorded by the SwisensPoleno, transformation from pixel to μm was necessary. For this the theoretical image resolution of

0.595 $\mu\text{m}/\text{px}$ was used. The size calculation is influenced by a relative size-overestimation of the holographic images, which is lower for larger particles. Additionally, the size estimation can be influenced by poorly focused particles and difficult differentiation between particle and image background. This mostly for smaller particles, which also tend to be brighter. The result is a pronounced overestimation, which decreases drastically above 5 μm . This effect has been noted, but not compensated in the presented data, as the same estimations are true for all four aerosol generators and has no major impact in the allocation of the particles in the size categories.

The recorded particles were categorized according to several parameters calculated from image properties (Li, Wilkinson, and Patchigolla 2005). The equivalent circular area diameter D_A is calculated from the area A occupied by the particle in the holographic image upon transformation into a circle with the same area A :

$$D_A = 2 \cdot \sqrt{\frac{A}{\pi}}$$

The equivalent circular perimeter diameter D_P , is calculated from the perimeter P of the silhouette of the measured particle upon transformation into a circle with the same perimeter P :

$$D_P = \frac{P}{\pi}$$

Assuming that chains of spores and aggregates are also produced and measured, the particles were categorized according to their shape, as this can have an impact on their behavior in the human respiratory tract (Finlay 2021). For this classification, the following characteristic values were determined from the holography images: major and minor axis as well as sphericity (S). Based on the minor and major axis, the particles were classified as spore chains (minor $<10 \mu\text{m}$, major $>20 \mu\text{m}$) or round particles. We assume that roundish particles include single spores, small groups of spores and agglomerates in different sizes. To evaluate how round the particles are, the sphericity (Li, Wilkinson, and Patchigolla 2005) was calculated from the ratio of D_A to D_P :

$$S = \left(\frac{D_A}{D_P} \right)$$

Sphericity provides an estimate of the roundness of a particle, i.e., how closely it matches a sphere.

These parameters were calculated for each holographic image of the data set. To capture all particles, the SwisensPoleno Jupiter instruments were operated with the highest sensitivity. However, this can lead to images

with no particles in them, which can be artifacts, too small particles or occur due to bad focus. These images can be identified based on the intensity of the recorded pixels. To filter these, the difference between the maximum and minimum grayscale intensity of all pixels in both images is determined. If the intensity difference is less than 10% of the pixel grayscale intensity range, the measurement events were labeled as “Empty images.” Very small ($<4 \mu\text{m}$) and very bright particles will cause the image analysis to fail. As a result, the characteristic values determined from the images are not meaningful and distort the results. Therefore, such measurement data were labeled as unknown particles. After filtering these images and particles out of the datasets, the remaining data points were considered microbial particles in this study. This filtering was especially relevant for the data derived by the tests with the LSA, as is described in the results section.

Based on their size (D_A) and shape, the microbial particles were classified in different categories. The size categories were chosen to match the ranges important for penetration of the regions of the human lung, where over 20 μm are not inhalable and 20 μm to 1 μm are inhalable (Brown et al. 2013). Depending on the size, the particles are expected to deposit in different regions of the respiratory tract (Sierra-Vargas and Teran 2012; Löndahl 2014; Lazaridis 2023). To relate the produced bioaerols by the generators to the depositions, we grouped them in the following categories: $>20 \mu\text{m}$ (lower probability of deposition in mouth and nose, about 30%), 20–9 μm (high probability of deposition in mouth and nose, over 30%), 9–5 μm (probable deposition in tracheobronchial region), <5 (probable deposition in alveolar region). In addition to the size (D_A) and shape (S) categorization, randomly chosen pictures were checked manually to ensure plausibility. No particles below 2 μm have been recorded, therefore this category is not shown in the results section and the smallest category defined as under 5 μm .

2.7. Data conversion for comparison of measurement instruments

To compare particle size distribution measured by the SwisensPoleno Jupiter and the Grimm 11-C the aggregated size counts from the 11-C were transformed with the inverse concentrator characteristic of the SwisensPoleno (Figure S1). The reason for this is the integrated aerosol particle concentrator of the SwisensPoleno Jupiter, which concentrates particles above 10 μm by a factor of up to 1000 following a function of particle size. For the transformation it was assumed that the particles have a density of $0.6 \frac{\text{kg}}{\text{m}^3}$.

In order to compare magnitudes from an imaging method with a scattered light measurement method, a conversion method was used utilizing the analysis of the equivalent area diameter (D_A) and the sphericity (S) of the particle image (Li, Wilkinson, and Patchigolla 2005). The conversion was applied to the measurement data of the SwisensPoleno Jupiter and done for both holographic images separately. To have a single key value for each particle the mean of the equivalent diameter from both sides of the particle was calculated:

$$Size_{LD} = \sqrt{S} \cdot D_A$$

Besides the equivalent diameter the major and minor axis of the ellipse with the same central moments as the particle were analyzed (van der Walt et al. 2014).

3. Results

In the study presented here, we tested four bioaerosol generators using three fungal organisms and two SwisensPoleno Jupiter real-time particle characterization instruments. For each combination of aerosol generator, fungal organism and sampling instrument, at least 6000 particles were recorded. To compare the produced aerosols of the aerosol generators, we analyzed the produced particle number concentrations, the particle size distribution and the dependence of the particle shapes on the dispersal method.

3.1. Particle concentrations in test aerosols

As the tested aerosol generators use different principles for the production of bioaerosols, as well as different aerosol- or mixing chambers, the concentration of spores delivered to the SwisensPoleno Jupiter instruments differed between the aerosolization methods. Therefore, the

time to receive the required amount of data points was different. The RBG with its lowest setting delivered about 12000 to 17000 particles/ m^3 to the instrument. For the FAG and the SWA the reached output depends strongly on the chosen settings. For them up to 15000 to 16000 particles/ m^3 could be produced with the chosen settings, but also lower concentrations were possible. The setup with the LSA delivered between 2000 and 2500 particles/ m^3 to the SwisensPoleno Jupiter. All the data mentioned include all particles detected by the SwisensPoleno Jupiter before filtering out empty images and unknown particles (see the [online supplementary information](#)). The LSA for example produces small droplets in addition to solid particles, and thus were detected by the instrument but excluded later in post processing.

3.2. Size distribution of the particles

To evaluate the size of the particles produced by the different aerosolization methods, the equivalent area diameter D_A and the length of the major and minor axes of each particle, calculated by the SwisensPoleno software from the holographic image area.

The RBG and FAG produced the particles with the smallest D_A (Figure 2) and smallest axes (Figure 3) for all three test organisms. Calculated diameters closely resemble values for single spores published in literature from *Aspergillus brasiliensis*, but are slightly above published values for *Cladosporium cladosporioides* and *Tirchoderma longibrachiatum*. In both figures, individual spores should be represented in the low end of the x-axis, here the RBG shows the highest relative abundance for *A. brasiliensis*. For *C. cladosporioides* and *T. longibrachiatum*, beside the RBG, also the FAG has the highest proportion of particles in the bin where individual spores are expected. The SWA showed a slight shift to bigger

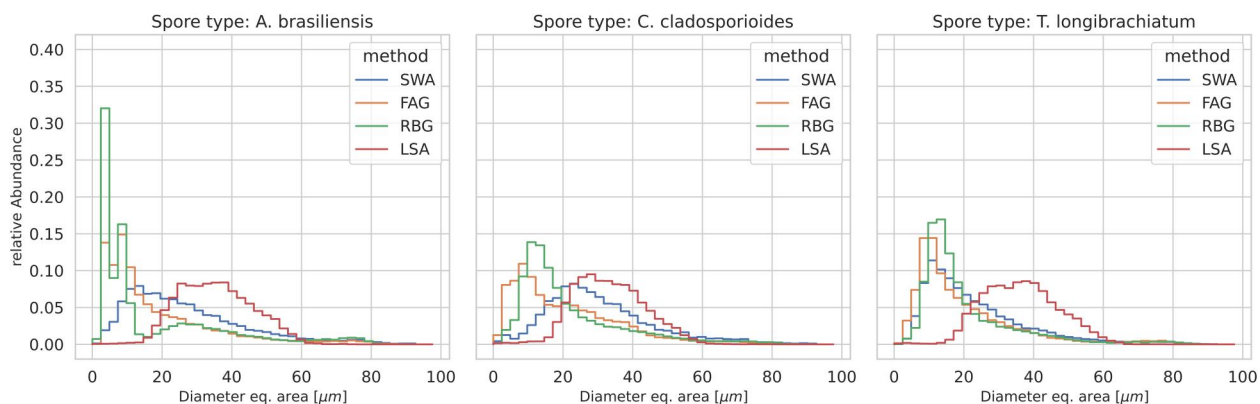


Figure 2. Particle size distribution calculated by equivalent area diameter, as relative abundance of all recorded particles, of each aerosolizer methods for three test organisms (*A. brasiliensis*, *C. cladosporioides*, *T. longibrachiatum*); SWA = SwisensAtomizer ($n = 21372, 8752, 21241$), FAG = fungal aerosol generator ($n = 22698, 13969, 27572$), RBG = rotating brush generator ($n = 20483, 20412, 22529$), LSA = liquid sparging aerosolizer ($n = 16623, 14628, 13257$).

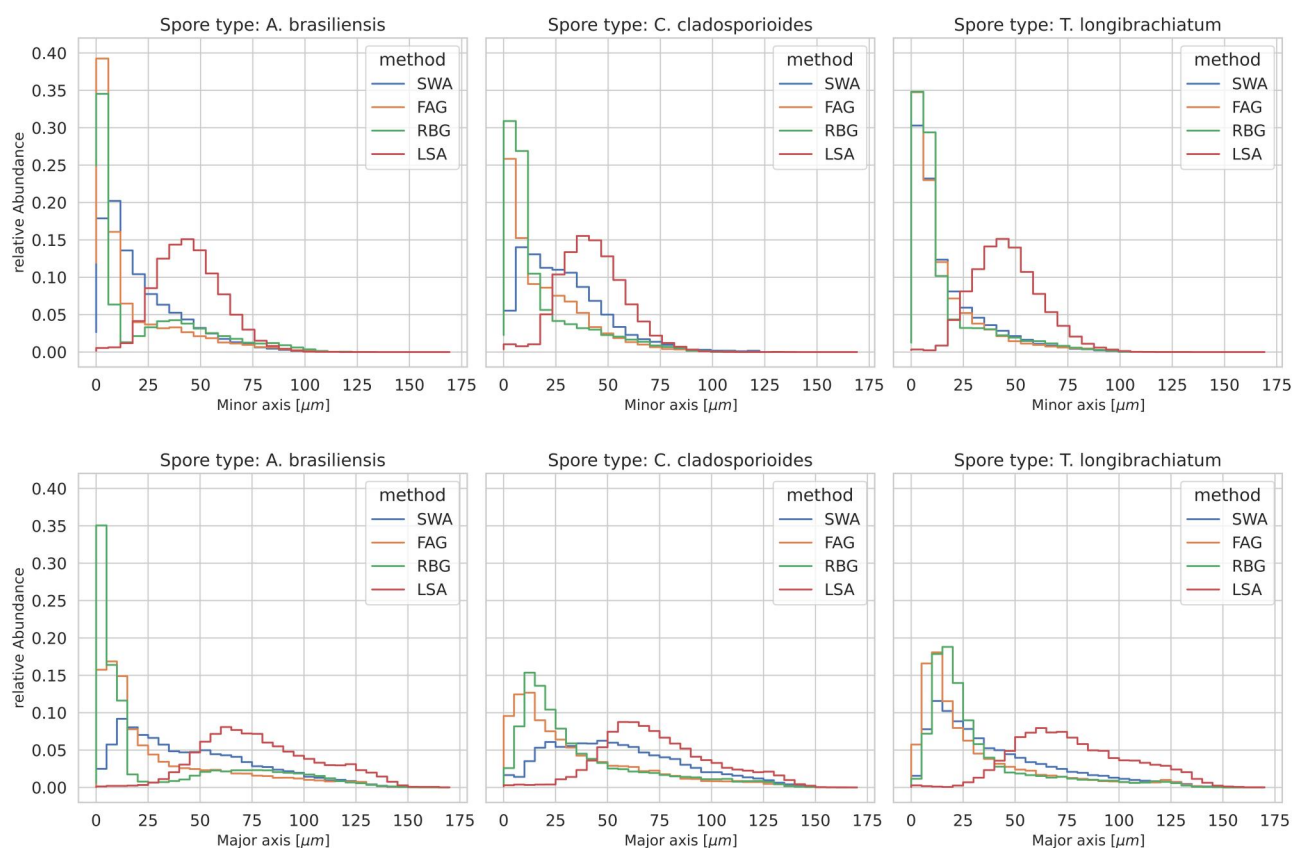


Figure 3. Distribution of the length of the major and minor axis, as relative abundance of all recorded particles produced by each aerosolizer methods for three test organisms (*A. brasiliensis*, *C. cladosporioides*, *T. longibrachiatum*); SWA = SwisensAtomizer ($n = 21372, 8752, 21241$), FAG = fungal aerosol generator ($n = 22698, 13969, 27572$), RBG = rotating brush generator ($n = 20483, 20412, 22529$), LSA = liquid sparging aerosolizer ($n = 16623, 14628, 13257$).

particles compared to the FAG and RBG, with the most overlap for *T. longibrachiatum*. For the LSA a high portion of big particles was recorded starting with $10\ \mu\text{m}$ diameter. These big particles between 20 and $60\ \mu\text{m}$ rather resemble droplets instead of single spores. When excluding the particles, defined as empty images and unknown particles, the remaining particles detected by the SwisensPoleno Jupiter are in the size range comparable to the other aerosolization methods (Figure 4). All aerosolizers have a wide particle size spectrum, which makes it clear that not only individual spores are produced, but also chains and agglomerates.

3.3. Shape distribution of the particles

The holographic images captured from two sides of the particle, represent the cross sectional area. Therefore, we were able to analyze roundness of the particles, using the sphericity and investigate differences between the aerosolization methods. Figure 5 shows that there is a difference in the particle sphericity depending on the used organism and aerosolizer. Similar to the results for D_A and length of axes, sphericity values

obtained upon aerosolization with the RBG and the FAG were similar for each spore type. The RBG combined with *A. brasiliensis* showed the biggest share of very round particles, with a sphericity around one. Only a minority of particles from *C. cladosporioides* showed a high sphericity upon aerosolization with the FAG, whereas the major part was shifted toward low a sphericity. The SWA generally resulted in particles with low sphericity, but particles with a more complex shape. This was especially clear for *A. brasiliensis* and *C. cladosporioides*. For the LSA the sphericity of most of the images was very low, but it must be considered, that these data include all images, including empty pictures and unknown particles, which also include data points presumed to be water droplets. According to the Figure S3, the majority of the particles measured with LSA are water droplets or unknown particles.

3.4. Classification as spore agglomerates and chains of microbial particles

As described, especially the particles produced by the LSA and their pictures recorded by the SwisensPoleno

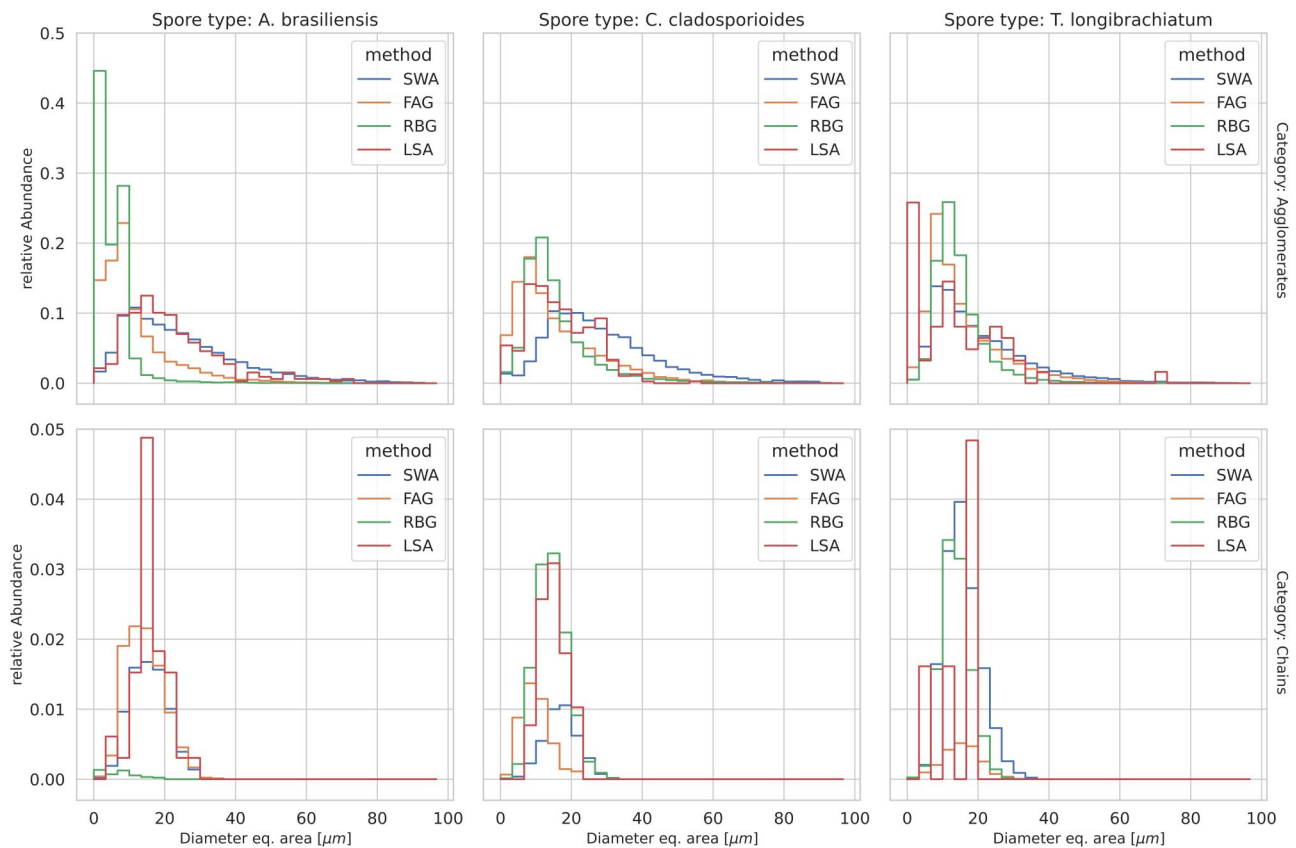


Figure 4. Size distribution of measured microbial particles classified as spore agglomerates (top) or chains (bottom), as relative abundance of each aerosolizer methods for three test organisms (*A. brasiliensis*, *C. cladosporioides*, *T. longibrachiatum*); y-axis are scaled differently for better readability; SWA = SwisensAtomizer ($n = 17311, 5230, 17518$), FAG = fungal aerosol generator ($n = 17123, 8972, 22517$), RBG = rotating brush generator ($n = 12774, 15125, 16856$), LSA = liquid sparging aerosolizer ($n = 328, 389, 62$).

Jupiter often showed unspecific particles, or no particles could be found on the pictures. After filtering the original data sets, for the types *A. brasiliensis*, *C. cladosporioides*, *T. longibrachiatum* this resulted in about 40000 to 49000 data points for the FAG, RBG and SWA and only under 800 for the LSA. These data

points are presumed to include microbial particles and were further analyzed by categorizing them according to their shape into spore chains and agglomerates.

Figure 4 shows that the proportion of chains is much smaller compared to agglomerates and round

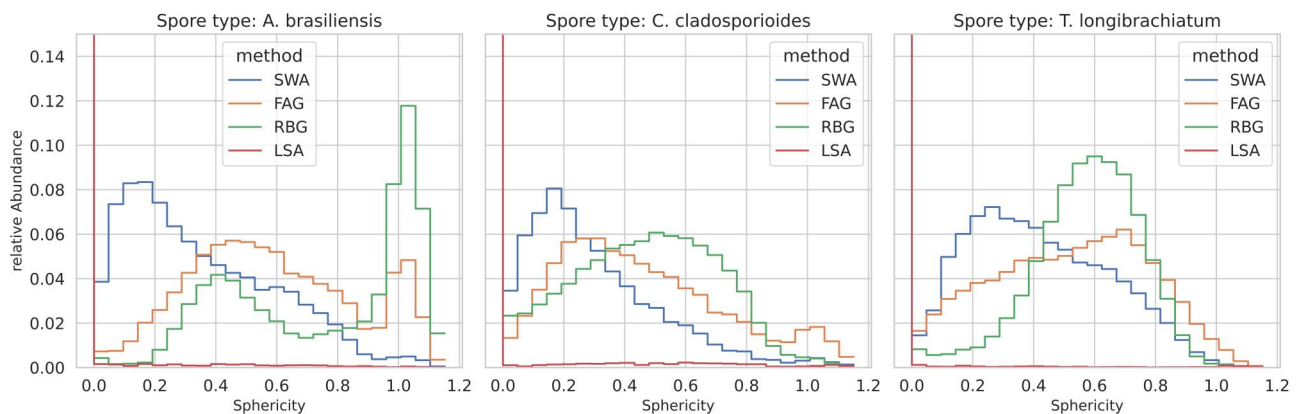


Figure 5. Distribution of the sphericity as relative abundance of all recorded particles, produced by each aerosolizer methods for three test organisms (*A. brasiliensis*, *C. cladosporioides*, *T. longibrachiatum*); SWA = SwisensAtomizer (21372, 8752, 21241), FAG = fungal aerosol generator ($n = 22698, 13969, 27572$), RBG = rotating brush generator ($n = 20483, 20412, 22529$), LSA = liquid sparging aerosolizer ($n = 16623, 14628, 13257$).

particles. Considering the size distribution of the chains, all organisms result in very similar size patterns, regardless of the aerosolization method. Again, as for the total particles, the RBG with *A. brasiliensis* produced the highest share of round particles, which were classified as small agglomerates. For *A. brasiliensis* the patterns of RBG and FAG fit well together, whereas for *T. longibrachiatum* also the SWA produced a similar distribution. For *A. brasiliensis* and *C. cladosporioides* the comparison of RBG and FAG with SWA, showed that the share of small particles of the SWA is smaller. The curve of the LSA data is deviant, as only a small number of data points is available.

3.5. Examination of sizes and shape of microbial particles

Based on the sphericity and the size (diameter), the particles were combined into categories ($<5\ \mu\text{m}$, $5\text{--}9\ \mu\text{m}$, $9\text{--}20\ \mu\text{m}$ and $\geq 20\ \mu\text{m}$, see Figure 6). Only for the combination LSA and *T. longibrachiatum* a recognizable share of particles could be found with a size below $5\ \mu\text{m}$. Considering each of the combinations of aerosolization method and organism separately, it is clear that the FAG produced the highest fraction of microbial particles in the size range of $9\text{--}20\ \mu\text{m}$ and the highest share of roundish particles in that size. The output of the RBG was highly influenced by the used material. For *A. brasiliensis* a higher portion of particles were between $5\text{--}9\ \mu\text{m}$ than for *T. longibrachiatum* and *C. cladosporioides*. The SWA produced the highest share of microbial particles larger than $20\ \mu\text{m}$. The particles produced by the LSA were mostly bigger than $9\ \mu\text{m}$, but considering the size range of 5 to $9\ \mu\text{m}$, a high portion of the particles had a sphericity close to one, being most probable single spores. Especially in the size range of $\geq 20\ \mu\text{m}$ the graphs for the LSA shows quantization artifacts, as for this aerosol generator a lower number of particles was used for the analysis due to excessive filtering. In general, the data shows, that the bigger the recognized particles were, the farther away they are from a sphericity of 1.

3.6. Comparison of particle size of the SwisensPoleno Jupiter and the grimm 11-C

As the SwisensPoleno Jupiter is a new method to evaluate fungal airborne particles, we compared the detected particles with the particle concentration recorded by a light scattering particle spectrometer, while the RBG was used to produce aerosols inside the CCB3000. The SwisensPoleno sizes and the

Grimm 11-C counts were transformed (see 2.7) and the SwisensPoleno data was binned according to the size channels of the Grimm 11-C. Figure 7 shows that for *C. cladosporioides* the agreement of the two instruments fits very well. For *A. brasiliensis*, a shift between SwisensPoleno Jupiter and Grimm 11-C can be seen, where the Grimm 11-C recognized more small particles and the SwisensPoleno Jupiter more particles between 5 and $10\ \mu\text{m}$. Also for *T. longibrachiatum* a slight shift can be seen, but far less than for *A. brasiliensis*. This could be due to a higher overestimation of the particle size by the SwisensPoleno Jupiter for smaller particles. Also, the instrument is more sensitive to bigger particles, therefore the recognition of smaller particles is reduced. In summary, the data shows that for the higher particle sizes, the two instruments fit very well together, whereas for small particles the sensitivity of the SwisensPoleno Jupiter is lower in the total particle number recognition.

4. Discussion and outlook

The goal of the study presented here was to characterize the fungal aerosol produced by four different aerosol generators with a new real-time detection method, enabling detailed analysis of the airborne particles. Our results show that the particles produced differ in concentration, size and shape, depending on the used aerosolization method and fungal organism.

The detection system, of course, also has an influence on the obtained data. Real-time instruments were also used in other studies for testing of bioaerosol generators (Jung et al. 2009), where the instrument was a particle size distribution analyzer (PSD 3603). With that instrument, no subsequent inspection and analysis of the particles is possible after data collection. On basis of the holographic imaging of the SwisensPoleno Jupiter, the particles can be further analyzed after the experiment and spot-checked by microscopy specialists. Another potential advantage is the combination of holographic imaging and the use of the fluorescence measurement data from the SwisensPoleno Jupiter for the detection of fungal particles.

As previous studies already showed, it is possible to discriminate between various biological particles like pollen, fungal spores and bacteria, based on their fluorescent profile recorded by single-particle fluorescence detection (Pan 2015). Furthermore, the possibility of discriminating different shapes of particles by machine learning algorithms has been tested previously in a simulation study (Piedra et al. 2019). A

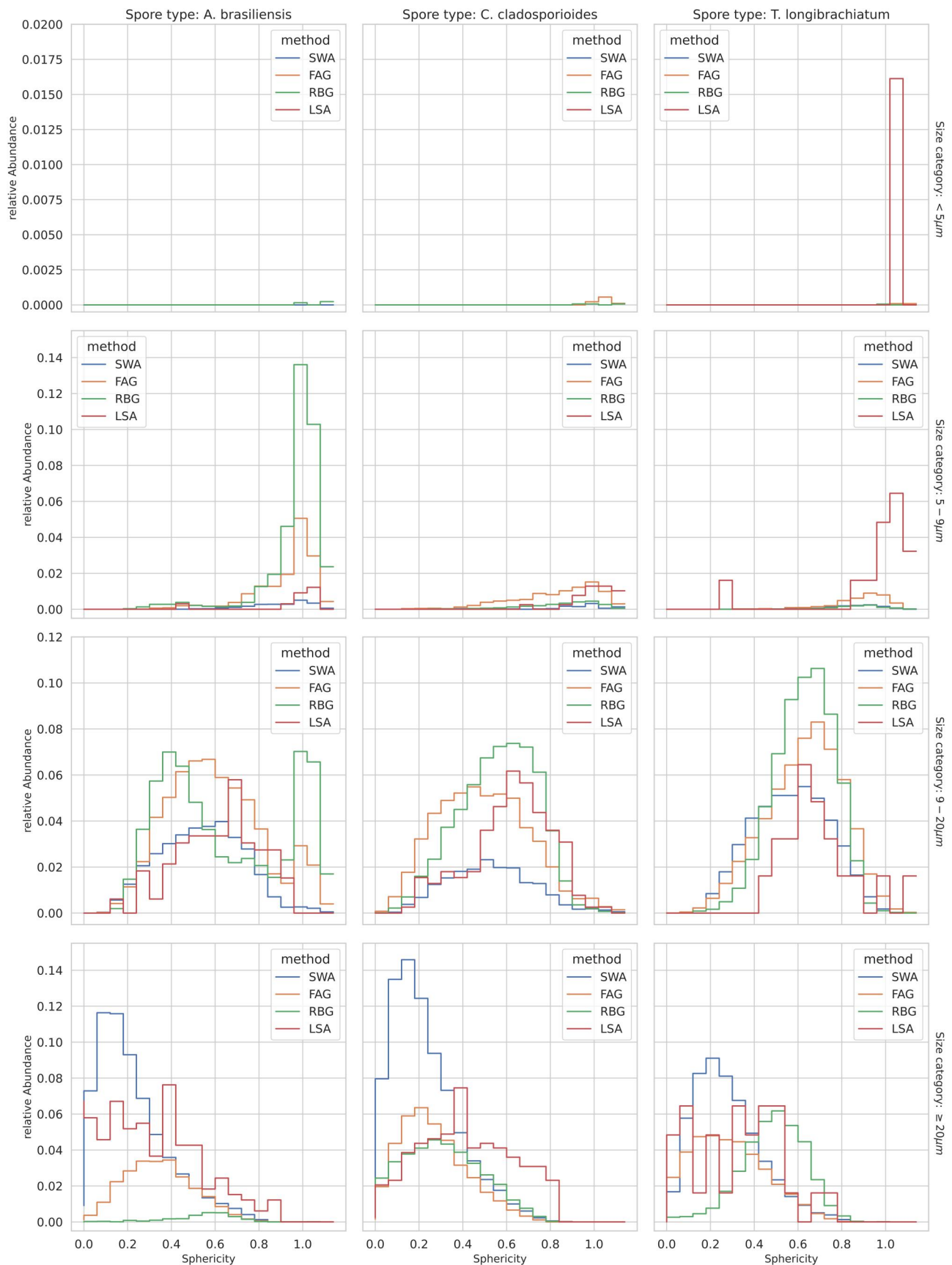


Figure 6. Different size categories, as relative abundance of microbial particles of each aerosolizer method, plotted against the particles sphericity, for all three test organisms (*A. brasiliensis*, *C. cladosporioides*, *T. longibrachiatum*); SWA = SwisensAtomizer ($n = 17311, 5230, 17518$); y-axis are scaled differently for better readability; FAG = fungal aerosol generator ($n = 17123, 8972, 22517$), RBG = rotating brush generator ($n = 12774, 15125, 16856$), LSA = liquid sparging aerosolizer ($n = 328, 389, 62$).

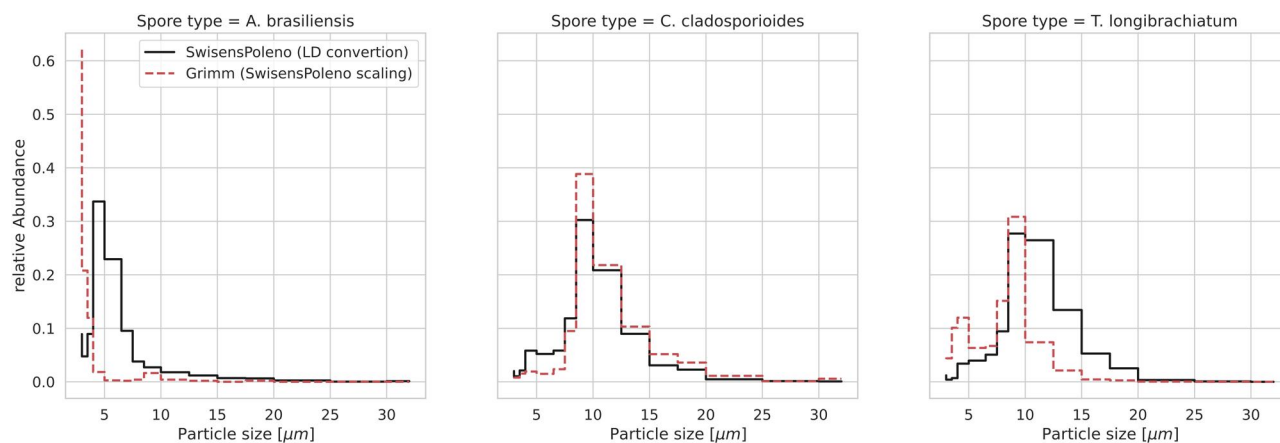


Figure 7. Comparison of the size of all measured particles, calculated by the SwisensPoleno Jupiter and the optical particle counter Grimm 11-C, depicted for all three test organisms, produced by the RBG and measured by both instruments, side by side in the aerosol chamber CCB3000.

recent study by the Lucerne University of Applied Sciences and Arts (HSLU), (ASMO – Advanced Spore Monitoring) showed that with the SwisensPoleno Jupiter, it is possible to differentiate between different fungal taxa according to their fluorescence profile (data in preparation for publication). In principle, it is possible that the different aerosol generators as well as the preparation of the source material, also influence the fluorescence profile of the microbial particles produced. These analyses have not been done yet on the here presented data, however, and need to be done in the future.

Comparing the four aerosolization methods, the produced concentration varied, giving the highest output by the RBG, with a high share of small and round particles, especially for *A. brasiliensis*. Although the total concentration was not as high, the FAG showed very similar patterns in microbial particle size, shape and distribution for all three test organisms. For *C. Cladosporioides* the FAG produced more very small agglomerates assumed as single spores than the RBG. For the FAG, the size and shape of produced particles can be adjusted by the air flow of pressured air, used to generate the aerosol (Lee et al. 2010). In the presented study, only one setting was used for all fungal taxa and repetitions and this potential for optimization not further investigated. The SWA produced a high share of non-spheric, rather large particles. This may be due to the clustering of spores together in the dust and low shear forces in the aerosol production by vibration and airflow. The lowest concentration of particles, and especially as microbial classified ones was produced by the LSA. Although a high concentration of spores in the suspension was used, the concentration was limited to a few thousand particles per m^3 . This can be mainly attributed to a concentration

plateau, as has been previously described (Mainelis et al. 2005; Dellinger 2020). Additionally a high percentage, up to 90%, of non-spore particles, depending on the size category was recognized. We assume that not fully dried small droplets reached the sampling area, but are too small to be recognized as particles by image processing. The microbial data, which includes the chains and agglomerates, showed a recognizable number of particles below 5 μm only for the LSA.

Comparing the SwisensPoleno Jupiter with the Grimm 11-C, especially for *Aspergillus brasiliensis*, more particles below 5 μm could be recognized with the later, suggesting an underestimation of this size range by the SwisensPoleno Jupiter. This under recognition of small particles may be the reason for the low concentration recognized from aerosolization with the LSA, as this aerosolizer is built to mainly produce single spore aerosols, which would be in the range of 3 to 7 μm .

The underestimation of small particles by the SwisensPoleno Jupiters can be explained, as particles larger than 10 μm are concentrated almost up to 1000 times, to improve the time resolution of the concentration determination of large particles such as pollen. In turn, this means that the counting efficiency for smaller particles is reduced. Additionally, the mechanisms of particle recognition and size calculation of the SwisensPoleno Jupiter and the Grimm 11-C are particularly different. Where the first uses holographic imaging, where an interference pattern is recognized by a camera and algorithm based image reconstruction is used to obtain the holographic image. In comparison, the later uses light-scattering, where the particle is illuminated by a laser and the mie dispersion is recognized. To obtain the particle size, the outline of the holographic image is recognized, the area calculated and compared to the area of a sphere to obtain the diameter of the particle in pixel. A

subsequent transformation into micrometer is necessary. For light scattering a calibration to spherical particles with known diameter is used, assigning the specific peak to the recognized dispersion. These differences may result in different size recognition of particles and size classification of complex aggregates. Furthermore, the size calculation of the SwisensPoleno Jupiter is influenced by a halo around particle images, and very small ($<5\mu\text{m}$) and bright particles may not be recognized at all.

The shape and size distribution as well as the reachable concentration range influence the possible applications of an aerosol generator. Based on the measured spores with the Hirst method, it is assumed that individual spores are relevant for natural dispersal outdoors. For training and evaluation of real-time detection instruments, therefore, the spores should be in the air as individually as possible. According to literature, the ideal setup for this application would be particles with the following characteristics: *A. brasiliensis* round particles in the range $3.5\text{--}4.5\mu\text{m}$, *C. cladosporioides*, conical particles in the range $2.5\text{--}3\mu\text{m}$ or $3\text{--}3.5\mu\text{m}$ and *T. longibarchiatum* round particles in the range $2.5\text{--}5\mu\text{m}$ (Bensch et al. 2010; Dannemiller et al. 2014). In summary for this application the generators should only generate particles that are smaller than $5\mu\text{m}$. Our investigations show that the methods used are not ideal but can still be used for this purpose, if the measurement system provides sufficient information about the individual particles. Thanks to the diverse measurement values of the SwisensPoleno, the measurement data can be filtered to generate training data sets containing individual spores. To fully evaluate the similarity between the produced aerosols and real life bioaerosol, data and images from spores from outdoor, indoor and occupation environments would be needed. A recent study already showed, that it is possible to detect *Alternaria* spores with the SwisensPoleno Jupiter (Erb et al. 2023). Further studies, with smaller fungal spores in outdoor environments would be needed. For occupational settings, aerosolization mechanisms may differ from nature-based ones, as other forces lead to the dispersion of the particles. Until now, there is limited knowledge about the size or shape of the produced particles in various occupational settings.

Besides the presented results for the aerosol generators, also the influence of the preparation of the material has to be considered when evaluating the usability of the aerosol generators for a specific study (Alsved et al. 2020). As the FAG uses fungal colonies without any further manipulation, only the matter of an artificial growth media, lab conditions and monoculture are

obvious influences compared to nature. The LSA's principle of dispersion of spores through water can occur in nature, but is not presumed as the relevant dispersion mechanism for common airborne taxa like *Aspergillus*, *Cladosporium* and *Trichoderma* (McCartney 1994; Li, Liu, and Yao 2022). Also, the residence time of the spores in the liquid can alter the spores, for example regarding their size (Reponen et al. 2001). Furthermore, the chosen buffer could influence the properties of the spore aerosol or the detection method. In the course of dust production, the spores of *Trichoderma* and *Cladosporium* for this study have been freeze dried, to reduce the liquid. In later work, also the drying of media plates and collection of dust, like for *Aspergillus brasiliensis*, has been tested for other taxa (unpublished data). A comparison of freeze dried to heat dried material could give new insight into the impact of the dust production method. In general, airborne dispersal of dry spores is common in nature and of high relevance in indoor environments with mold growth (Li, Liu, and Yao 2022).

As a result, the data and differences in airborne microbial particles presented here, are a combination of the used material and the aerosolization method. Each step of bioaerosol generation, i.e., preparation and storage of material, aerosol generation and characterization, is critical for the interpretation of data (Alsved et al. 2020). In future investigations of bioaerosol generators, the combination of different detection methods, like real-time particle counters, holographic images as well as classical sampling on microscopic slides, filters and on media for subsequent culturing would give the most information about the advantages and disadvantages of the aerosol generation method.

Acknowledgments

Thanks to the laboratory team of AIT for help in producing the fungal spore dust, especially Lena Piglmann and Marija Gumze. Special thanks to Christian Amsüss for support and reviewing work.

Disclosure statement

The present scientific study was carried out in collaboration with the company SWISENS AG within the framework of research cooperation. SWISENS AG is a company that specializes in the development of solutions for aerosol particle measurement. The employees of the company, Mr. Erny Niederberger (position: Managing Director) and Mr. Elias Graf (position: Application Engineer), actively participated in the study. Mr. Erny Niederberger assisted in the design of the study and Mr. Elias Graf assisted in the data analysis. It should be noted that there are potential conflicts of interest as SWISENS AG develops and distributes the

SwisensPoleno Jupiter measurement instruments, which is related to the topic of the study. However, Swisens AG considers the independence of the researchers to be essential and has not taken any influence to embellish any results.

Funding

This work was co-funded by Innosuisse and MeteoSwiss. Swisens and AIT supported the study by providing labor contributions.

References

- Alsved, M., L. Bourouiba, C. Duchaine, J. Löndahl, L. C. Marr, S. T. Parker, A. J. Prussin, II, and R. J. Thomas. 2020. Natural sources and experimental generation of bioaerosols: Challenges and perspectives. *Aerosol Sci. Technol.* 54 (5):547–71. doi: [10.1080/02786826.2019.1682509](https://doi.org/10.1080/02786826.2019.1682509).
- Bensch, K., J. Z. Groenewald, J. Dijksterhuis, M. Starink-Willemse, B. Andersen, B. A. Summerell, H.-D. Shin, F. M. Dugan, H.-J. Schroers, U. Braun, et al. 2010. Species and ecological diversity within the *Cladosporium cladosporioides* complex (Davidiellaceae, Capnodiales). *Stud. Mycol.* 67:1–94. doi: [10.3114/sim.2010.67.01](https://doi.org/10.3114/sim.2010.67.01).
- Brown, J. S., T. Gordon, O. Price, and B. Asgharian. 2013. Thoracic and respirable particle definitions for human health risk assessment. *Part. Fibre Toxicol.* 10 (1):12. doi: [10.1186/1743-8977-10-12](https://doi.org/10.1186/1743-8977-10-12).
- Buters, J., B. Clot, C. Galán, R. Gehrig, S. Gilge, F. Hentges, D. O'Connor, B. Sikoparija, C. Skjoth, F. Tummon, et al. 2022. Automatic detection of airborne pollen: An overview. *Aerobiologia*. doi: [10.1007/s10453-022-09750-x](https://doi.org/10.1007/s10453-022-09750-x).
- CEN (European committee for standardization), TC 137, Technical committee Assessment of workplace Exposure, WG5, Work group Measurement of biological Agents. 2021. *EN14583:2020 - Workplace exposure - Volumetric bioaerosol sampling devices - General requirements for evaluation of performance and use*.
- Danelli, S. G., M. Brunoldi, D. Massabò, F. Parodi, V. Vernocchi, and P. Prati. 2021. Comparative characterization of bio-aerosol nebulizers in connection to atmospheric simulation chambers. *Atmos. Meas. Tech.* 14 (6): 4461–70. doi: [10.5194/amt-14-4461-2021](https://doi.org/10.5194/amt-14-4461-2021).
- Dannemiller, K. C., N. Lang-Yona, N. Yamamoto, Y. Rudich, and J. Peccia. 2014. Combining real-time PCR and next-generation DNA sequencing to provide quantitative comparisons of fungal aerosol populations. *Atmos. Environ.* 84:113–21. doi: [10.1016/j.atmosenv.2013.11.036](https://doi.org/10.1016/j.atmosenv.2013.11.036).
- Dellinger, L. 2020. Bioaerosol generators- characteristics, impact on organisms and areas of application. Bachelor Thesis, Austrian Biotech University of applied sciences.
- Douwes, J., P. Thorne, N. Pearce, and D. Heederik. 2003. Bioaerosol health effects and exposure assessment: Progress and prospects. *Ann. Occup. Hyg.* 47 (3):187–200. doi: [10.1093/annhyg/meg032](https://doi.org/10.1093/annhyg/meg032).
- Druzhinina, I. S., M. Komoń-Zelazowska, L. Kredics, L. Hatvani, Z. Antal, T. Belayneh, and C. P. Kubicek. 2008. Alternative reproductive strategies of *Hypocrea orientalis* and genetically close but clonal *Trichoderma longibrachiatum*, both capable of causing invasive mycoses of humans. *Microbiology (Reading)* 154 (Pt 11):3447–59. doi: [10.1099/mic.0.2008/021196-0](https://doi.org/10.1099/mic.0.2008/021196-0).
- Erb, S., A. Berne, N. Burgdorfer, B. Clot, M.-J. Graber, G. Lieberherr, C. Sallin, F. Tummon, and B. Crouzy. 2023. Automatic real-time monitoring of fungal spores: The case of *Alternaria* spp. *Aerobiologia*. doi: [10.1007/s10453-023-09780-z](https://doi.org/10.1007/s10453-023-09780-z).
- European Commission - Enterprise and industry directorate-general. 2008. Volume4: EU Guidelines to Good Manufacturing Practice, Medical Products for Human and Veterinary Use - Annex 1 Manufacture of Sterile Medicinal Products. EudraLex - The Rules Governing Medicinal Products in the European Union, 1–16.
- Finlay, W. H. 2021. Deposition of aerosols in the lungs: Particle characteristics. *J. Aerosol Med. Pulm. Drug Deliv.* 34 (4):213–6. doi: [10.1089/jamp.2021.29040.whf](https://doi.org/10.1089/jamp.2021.29040.whf).
- Ghosh, B., H. Lal, and A. Srivastava. 2015. Review of bio-aerosols in indoor environment with special reference to sampling, analysis and control mechanisms. *Environ. Int.* 85:254–72. doi: [10.1016/j.envint.2015.09.018](https://doi.org/10.1016/j.envint.2015.09.018).
- Górny, R. L., T. Reponen, K. Willeke, D. Schmechel, E. Robine, M. Boissier, and S. A. Grinshpun. 2002. Fungal fragments as indoor air biocontaminants. *Appl. Environ. Microbiol.* 68 (7):3522–31. doi: [10.1128/AEM.68.7.3522](https://doi.org/10.1128/AEM.68.7.3522).
- Gunnbjörnsdóttir, M. I., D. Norbäck, P. Plaschke, E. Norrman, E. Björnsson, and C. Janson. 2003. The relationship between indicators of building dampness and respiratory health in young Swedish adults. *Respir. Med.* 97 (4):302–7. doi: [10.1053/rmed.2002.1389](https://doi.org/10.1053/rmed.2002.1389).
- Hasegawa, N., S. Yamasaki, and Y. Horiguchi. 2011. A study of bacterial culturability during bioaerosol challenge test using a test chamber. *J. Aerosol Sci.* 42 (6):397–407. doi: [10.1016/j.jaerosci.2011.02.009](https://doi.org/10.1016/j.jaerosci.2011.02.009).
- Hatvani, L., M. Homa, K. Chenthamara, F. Cai, S. Kocsubé, L. Atanasova, E. Mlinaric-Missoni, P. Manikandan, R. Revathi, I. Dóczy, et al. 2019. Agricultural systems as potential sources of emerging human mycoses caused by *Trichoderma*: a successful, common phylotype of *Trichoderma longibrachiatum* in the frontline. *FEMS Microbiol. Lett.* 366 (21):1–13. doi: [10.1093/femsle/fnz246](https://doi.org/10.1093/femsle/fnz246).
- Heo, K. J., H. B. Kim, and B. U. Lee. 2014. Concentration of environmental fungal and bacterial bioaerosols during the monsoon season. *J. Aerosol Sci.* 77:31–7. doi: [10.1016/j.jaerosci.2014.07.001](https://doi.org/10.1016/j.jaerosci.2014.07.001).
- Hirst, J. M. 1952. An automatic volumetric spore trap. *Ann. Appl. Biol.* 39 (2):257–65. doi: [10.1111/j.1744-7348.1952.tb00904.x](https://doi.org/10.1111/j.1744-7348.1952.tb00904.x).
- Huffman, J. A., A. E. Perring, N. J. Savage, B. Clot, B. Crouzy, F. Tummon, O. Shoshanim, B. Damit, J. Schneider, V. Sivaprakasam, et al. 2020. Real-time sensing of bioaerosols: Review and current perspectives. *Aerosol Sci. Technol.* 54 (5):465–95. doi: [10.1080/02786826.2019.1664724](https://doi.org/10.1080/02786826.2019.1664724).
- Jung, J. H., C. Ho Lee, J. Eun Lee, J. Hyun Lee, S. Soo Kim, and B. U. Lee. 2009. Design and characterization of a fungal bioaerosol generator using multi-orifice air jets and a rotating substrate. *J. Aerosol Sci.* 40 (1):72–80. doi: [10.1016/j.jaerosci.2008.09.002](https://doi.org/10.1016/j.jaerosci.2008.09.002).
- Kim, K., E. Kabir, and S. A. Jahan. 2018. Airborne bioaerosols and their impact on human health. *J. Environ. Sci. (China)* 67:23–35. doi: [10.1016/j.jes.2017.08.027](https://doi.org/10.1016/j.jes.2017.08.027).

- Konlechner, A., S. Goller, M. Gorfer, L. Mölter, and J. Strauss. 2013. Evaluierung einer Prüfkammer für Bioaerosolsammelsysteme. *Gefahrstoffe - Reinhaltung Der Luft* 73 (11/12):471–6.
- Lazaridis, M. 2023. Modelling approaches to particle deposition and clearance in the human respiratory tract. *Air Qual. Atmos. Health* 16 (10):1989–2002. doi: 10.1007/s11869-023-01386-1.
- Lee, J. H., G. B. Hwang, J. H. Jung, D. H. Lee, and B. U. Lee. 2010. Generation characteristics of fungal spore and fragment bioaerosols by airflow control over fungal cultures. *J. Aerosol Sci.* 41 (3):319–25. doi: 10.1016/j.jaerosci.2009.11.002.
- Liebers, V., M. Raulf-Heimsoth, and T. Brüning. 2008. Health effects due to endotoxin inhalation (review). *Arch. Toxicol.* 82 (4):203–10. doi: 10.1007/s00204-008-0290-1.
- Li, X., D. Liu, and J. Yao. 2022. Aerosolization of fungal spores in indoor environments. *Sci. Total Environ.* 820: 153003. doi: 10.1016/j.scitotenv.2022.153003.
- Li, M., D. Wilkinson, and K. Patchigolla. 2005. Comparison of particle size distributions measured using different techniques. *Particulate Sci. Technol.* 23 (3):265–84. doi: 10.1080/02726350590955912.
- Löndahl, J. 2014. *Bioaerosol detection technologies, bioaerosol detection technologies*. Edited by P. Jonsson, G. Olofsson, and T. Tjärnhage. New York, NY: Springer New York (Integrated Analytical Systems). doi: 10.1007/978-1-4419-5582-1.
- Löndahl, J., O. Nerbrink, N. Burman, T. Tjärnhage, C. Von Wachenfeldt, and U. Gosewinkel Karlson. 2012. Methods for generation of bioaerosol. In Nordic Aerosol Conference, NOSA, November 2012.
- Madsen, A. M., S. T. Larsen, I. K. Koponen, K. I. Kling, A. Barooni, D. G. Karottki, K. Tendal, and P. Wolkoff. 2016. Generation and characterization of indoor fungal aerosols for inhalation studies. *Appl. Environ. Microbiol.* 82 (8): 2479–93. doi: 10.1128/AEM.04063-15.
- Mainelis, G., D. Berry, H. Reoun An, M. Yao, K. DeVoe, D. E. Fennell, and R. Jaeger. 2005. Design and performance of a single-pass bubbling bioaerosol generator. *Atmos. Environ.* 39 (19):3521–33. doi: 10.1016/j.atmosenv.2005.02.043.
- Masotti, F., S. Cattaneo, M. Stuknytė, and I. De Noni. 2019. Airborne contamination in the food industry : An update on monitoring and disinfection techniques of air. *Trends in Food Sci. Technol.* 90 (June):147–56. doi: 10.1016/j.tifs.2019.06.006.
- McCartney, H. A. 1994. Dispersal of spores and pollen from crops. *Grana* 33 (2):76–80. doi: 10.1080/00173139409427835.
- Mudarri, D., and W. J. Fisk. 2007. Public health and economic impact of dampness and mold. *Indoor Air.* 17 (3): 226–35. doi: 10.1111/j.1600-0668.2007.00474.x.
- Oteros, J., E. Bartusel, F. Alessandrini, A. Núñez, D. A. Moreno, H. Behrendt, C. Schmidt-Weber, C. Traidl-Hoffmann, and J. Buters. 2019. Artemisia pollen is the main vector for airborne endotoxin. *J. Allergy Clin. Immunol.* 143 (1):369–77.e5. doi: 10.1016/j.jaci.2018.05.040.
- Pan, Y.-L. 2015. Detection and characterization of biological and other organic-carbon aerosol particles in atmosphere using fluorescence. *J. Quantitative Spectrosc. Radiative Transfer.* 150:12–35. doi: 10.1016/j.jqsrt.2014.06.007.
- Piedra, P., A. Kalume, E. Zubko, D. Mackowski, Y.-L. Pan, and G. Videen. 2019. Particle-shape classification using light scattering: An exercise in deep learning. *J. Quantitative Spectrosc. Radiative Transfer.* 231:140–56. doi: 10.1016/j.jqsrt.2019.04.013.
- Pogner, C., A. Konlechner, V. Unterwurzacher, A. Kolk, M. Hinker, L. Mölter, J. Strauss, M. Gorfer, and S. Strauss-Goller. 2019. A novel laminar-flow-based bioaerosol test system to determine biological sampling efficiencies of bioaerosol samplers. *Aerosol Sci. Technol.* 53 (4):355–70. doi: 10.1080/02786826.2018.1562151.
- Reponen, T., S. A. Grinshpun, K. L. Conwell, J. Wiest, and M. Anderson. 2001. Aerodynamic versus physical size of spores: Measurement and implication for respiratory deposition. *Grana* 40 (3):119–25. doi: 10.1080/00173130152625851.
- Samuels, G. J., A. Ismaiel, T. B. Mulaw, G. Szakacs, I. S. Druzhinina, C. P. Kubicek, and W. M. Jaklitsch. 2012. The longibrachiatum clade of trichoderma: a revision with new species. *Fungal Divers.* 55 (1):77–108. doi: 10.1007/s13225-012-0152-2.
- Sauvageat, E., Y. Zeder, K. Auderset, B. Calpini, B. Clot, B. Crouzy, T. Konzelmann, G. Lieberherr, F. Tummon, K. Vasilatou, et al. 2020. Real-time pollen monitoring using digital holography. *Atmos. Meas. Tech.* 13 (3):1539–50. doi: 10.5194/amt-13-1539-2020.
- Scheermeyer, E., and I. E. Agranovski. 2009. Design and evaluation of a new device for fungal spore aerosolization for laboratory applications. *J. Aerosol Sci.* 40 (10):879–89. doi: 10.1016/j.jaerosci.2009.06.003.
- Sharpe, R. A., N. Bearman, C. R. Thornton, K. Husk, and N. J. Osborne. 2013. Indoor fungal diversity and asthma: A meta-analysis and systematic review of risk factors. *J. Allergy Clin. Immunol.* 135 (1):110–22. doi: 10.1016/j.jaci.2014.07.002.
- Sierra-Vargas, M. P., and L. M. Teran. 2012. Air pollution : Impact and prevention. *Respirology* 17 (7):1031–8. doi: 10.1111/j.1440-1843.2012.02213.x.
- Simon, X., and P. Duquenne. 2013. Feasibility of generating peaks of bioaerosols for laboratory experiments. *Aerosol Air Qual. Res.* 13 (3):877–86. doi: 10.4209/aaqr.2012.12.0340.
- Soler, Z. M., and R. J. Schlosser. 2012. The role of fungi in diseases of the nose and sinuses. *Am. J. Rhinol. Allergy.* 26 (5):351–8. doi: 10.2500/ajra.2012.26.3807.
- Stockwell, R. E., E. L. Ballard, P. O'Rourke, L. D. Knibbs, L. Morawska, and S. C. Bell. 2019. Indoor hospital air and the impact of ventilation on bioaerosols : a systematic review. *J. Hosp. Infect.* 103 (2):175–84. doi: 10.1016/j.jhin.2019.06.016.
- Theisinger, S. M., O. De Smidt, and J. F. R. Lues. 2021. Categorisation of culturable bioaerosols in a fruit juice manufacturing facility. *PLoS One.* 16 (4):e0242969. doi: 10.1371/journal.pone.0242969.
- Thrane, U., S. B. Poulsen, H. I. Nirenberg, and E. Lieckfeldt. 2001. Identification of Trichoderma strains by image analysis of HPLC chromatograms. *FEMS Microbiol. Lett.* 203 (2):249–55. doi: 10.1016/S0378-1097(01)00361-5.
- Tummon, F., S. Adamov, B. Clot, B. Crouzy, M. Gysel-Beer, S. Kawashima, G. Lieberherr, J. Manzano, E. Markey, A. Moallemi, et al. 2021. A first evaluation of multiple

- automatic pollen monitors run in parallel. *Aerobiologia*. doi: [10.1007/s10453-021-09729-0](https://doi.org/10.1007/s10453-021-09729-0).
- Unterwurzacher, V., C. Pogner, H. Berger, J. Strauss, S. Strauss-Goller, and M. Gorfer. 2018. Validation of a quantitative PCR based detection system for indoor mold exposure assessment in bioaerosols. *Environ. Sci. Process. Impacts*. 20 (10):1454–68. doi: [10.1039/C8EM00253C](https://doi.org/10.1039/C8EM00253C).
- van der Walt, S., J. L. Schönberger, J. Nunez-Iglesias, F. Boulogne, J. D. Warner, N. Yager, E. Goullart, and T. Yu, Scikit-Image Contributors. 2014. scikit-image: image processing in Python. *Peer J* 2 (e453):e453. doi: [10.7717/peerj.453](https://doi.org/10.7717/peerj.453).
- Viegas, C., T. Faria, M. dos Santos, E. Carolino, A. Q. Gomes, R. Sabino, and S. Viegas. 2015. Fungal burden in waste industry: an occupational risk to be solved. *Environ. Monit. Assess.* 187 (4):199. doi: [10.1007/s10661-015-4412-y](https://doi.org/10.1007/s10661-015-4412-y).
- Walser-Reichenbach, S. M., J. Buters, R. Gorny, D. J. J. Heederik, S. Heinze, A. M. Madsen, H. Niculita-Hirzel, D. Nowak, E. Pieckova, M. Plaza, et al. 2020. Bioaerosol Expert Forum. *GrDL*. 80 (11–12):435–6. doi: [10.1186/s12948](https://doi.org/10.1186/s12948).
- Yamamoto, N., K. Bibby, J. Qian, D. Hospodsky, H. Rismani-Yazdi, W. W. Nazaroff, and J. Peccia. 2012. Particle-size distributions and seasonal diversity of allergenic and pathogenic fungi in outdoor air. *Isme J.* 6 (10): 1801–11. doi: [10.1038/ismej.2012.30](https://doi.org/10.1038/ismej.2012.30).
- Zhen, H., T. Han, D. E. Fennell, and G. Mainelis. 2014. A systematic comparison of four bioaerosol generators: Affect on culturability and cell membrane integrity when aerosolizing *Escherichia coli* bacteria. *J. Aerosol Sci.* 70: 67–79. doi: [10.1016/j.jaerosci.2014.01.002](https://doi.org/10.1016/j.jaerosci.2014.01.002).